Supplement of Atmos. Meas. Tech., 7, 3151–3175, 2014
http://www.atmos-meas-tech.net/7/3151/2014/
doi:10.5194/amt-7-3151-2014-supplement

Atmospheric Measurement Techniques Open Access

Supplement of

Satellite retrieval of aerosol microphysical and optical parameters using neural networks: a new methodology applied to the Sahara desert dust peak

M. Taylor et al.

Correspondence to: M. Taylor (patternizer@gmail.com)

Supplementary Material

S1 Assessment of the extrapolation potential of the CASE 4 NN

In order to assess the extent to which the range of values of the dataset at Dakar is captured by the range of values of the training dataset, Fig. S1 compares the minimum and maximum values of the target parameters in the training dataset of co-located and synchronous (MODIS+OMI/AERONET) Northern Africa sites with the values at Dakar.

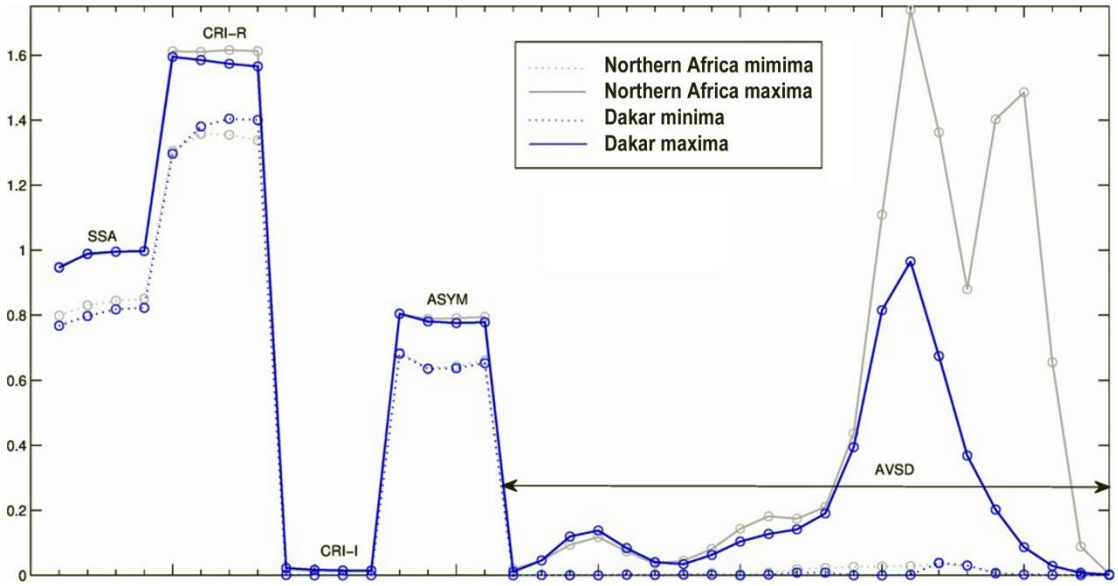

Figure S1. Comparison of the range of values of the target parameters in the training dataset of the CASE 4 NN constructed from co-located and synchronous (MODIS+OMI/AERONET) (grey) with those at Dakar (blue). Only (marginally) for the minimum values of the spectral SSA does the Dakar dataset extend outside the range of values of the training dataset at the Northern Africa sites. The CASE 4 NN is not therefore expected to have extrapolation potential.

S2 Daily retrieval of the AVSD

Figure 8 of the manuscript summarizes the quality of the daily retrieval of the AVSD. In Figs. S2.1-S2.14 below we present the daily AERONET Level 2 (Version 2) retrieval at Dakar with uncertainties as per the presentation in Taylor et al (2014) together with the NN retrieval using co-located and synchronous satellite inputs over Dakar. For each day, the AOD at 1020nm and the Pearson product-moment correlation coefficient (R) is given.

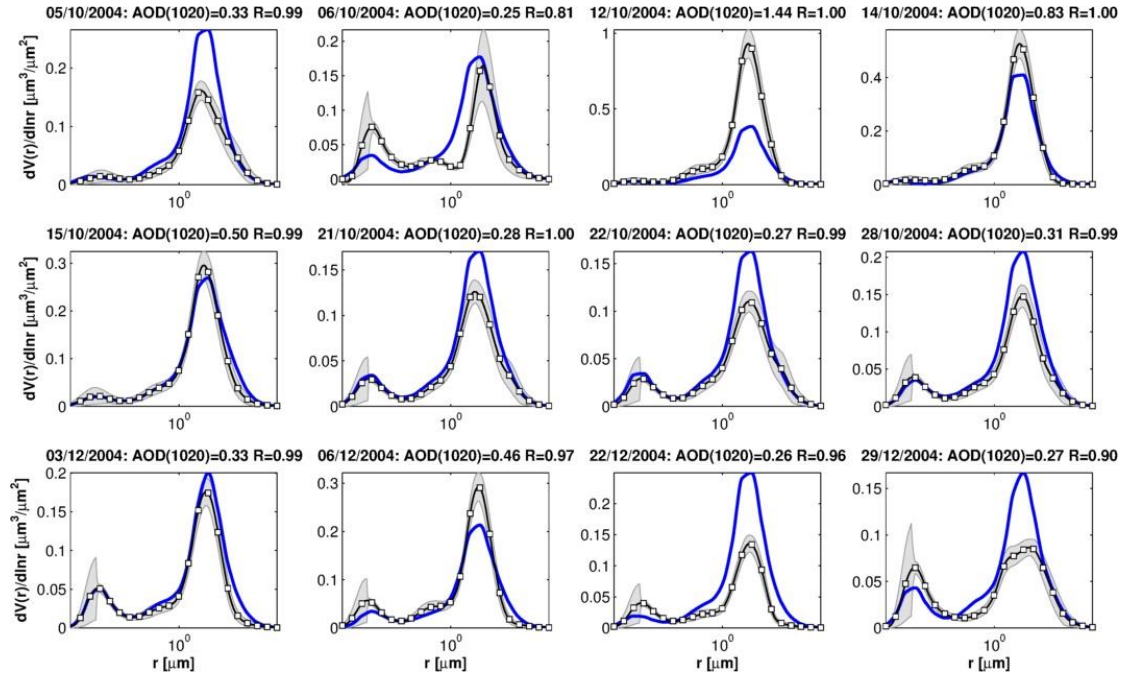

Figure S2.1. Comparison of the spline-fit NN retrieval (blue) and the AERONET daily AVSD retrieval at Dakar (squares overlaid on a spline-fit) for days 1-12 of the test dataset. The estimated error on the AERONET data is shown by the shaded grey band.

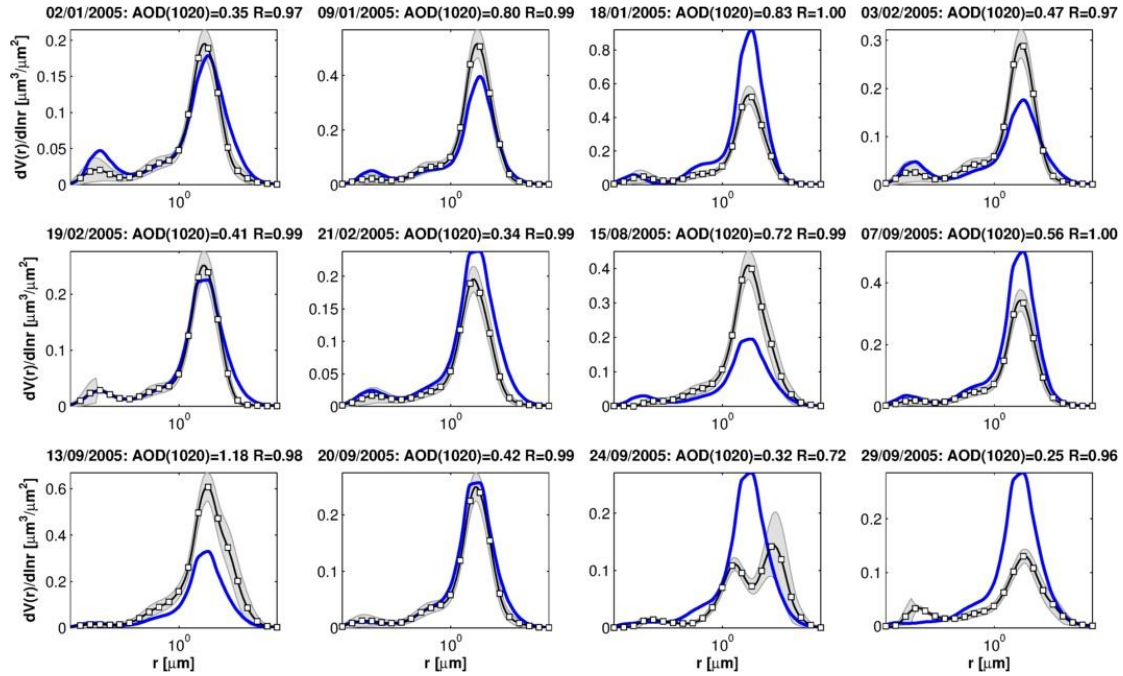

Figure S2.2. Comparison of the spline-fit NN retrieval (blue) and the AERONET daily AVSD retrieval at Dakar (squares overlaid on a spline-fit) for days 13-24 of the test dataset. The estimated error on the AERONET data is shown by the shaded grey band.

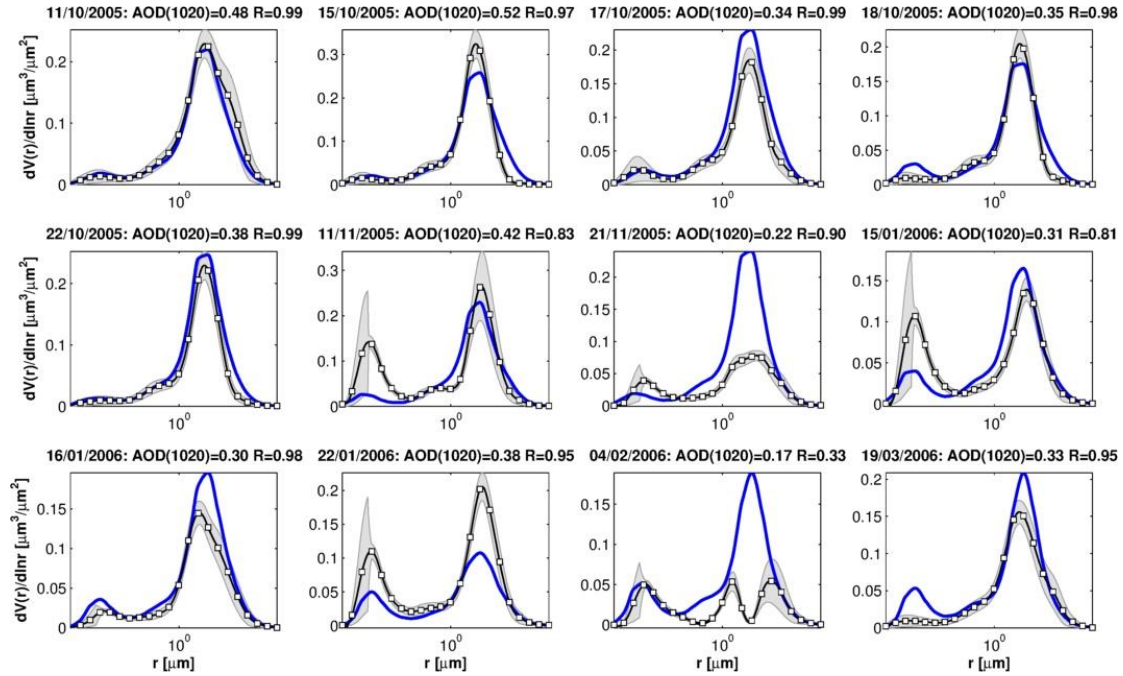

Figure S2.3. Comparison of the spline-fit NN retrieval (blue) and the AERONET daily AVSD retrieval at Dakar (squares overlaid on a spline-fit) for days 25-36 of the test dataset. The estimated error on the AERONET data is shown by the shaded grey band.

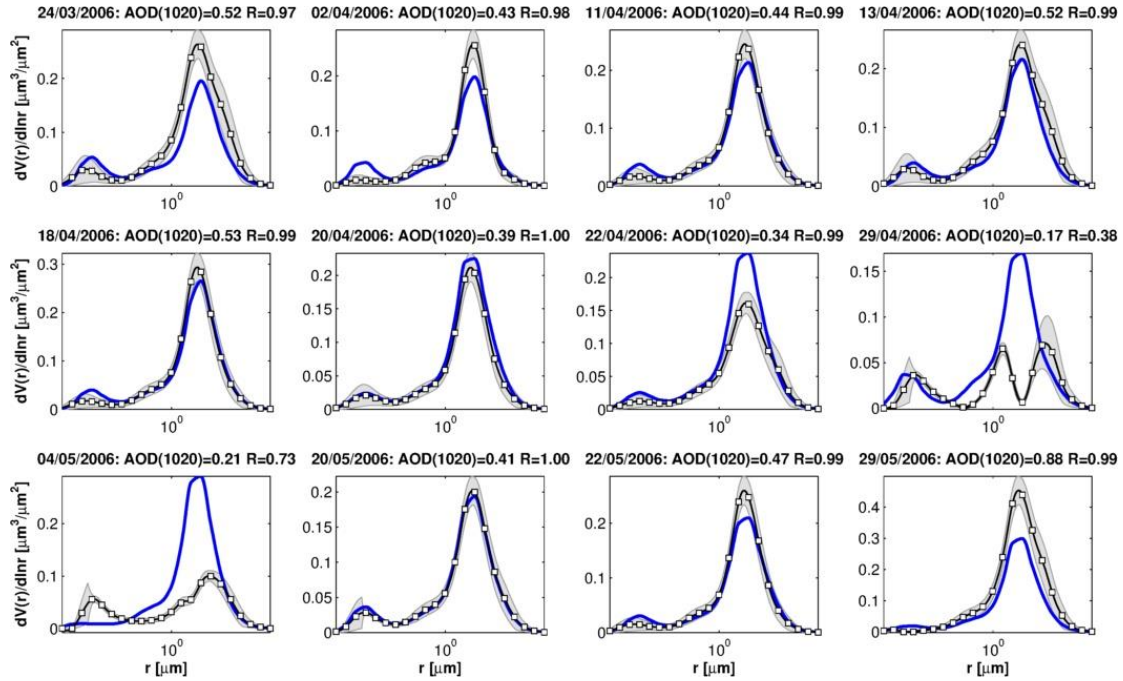

Figure S2.4. Comparison of the spline-fit NN retrieval (blue) and the AERONET daily AVSD retrieval at Dakar (squares overlaid on a spline-fit) for days 37-48 of the test dataset. The estimated error on the AERONET data is shown by the shaded grey band.

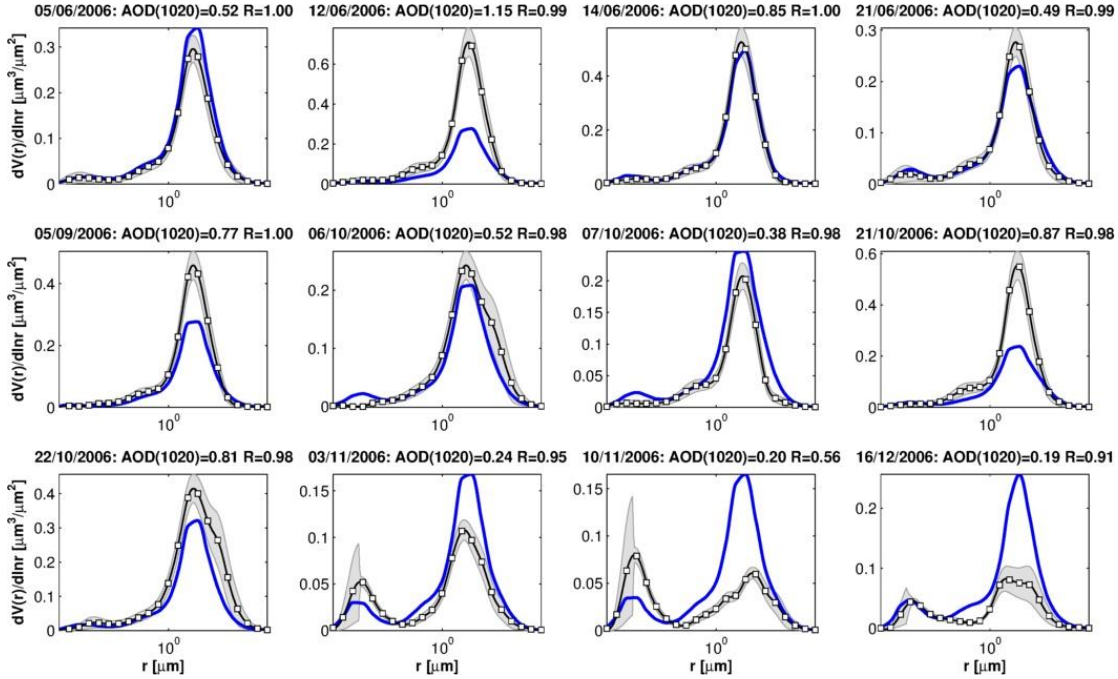

Figure S2.5. Comparison of the spline-fit NN retrieval (blue) and the AERONET daily AVSD retrieval at Dakar (squares overlaid on a spline-fit) for days 49-60 of the test dataset. The estimated error on the AERONET data is shown by the shaded grey band.

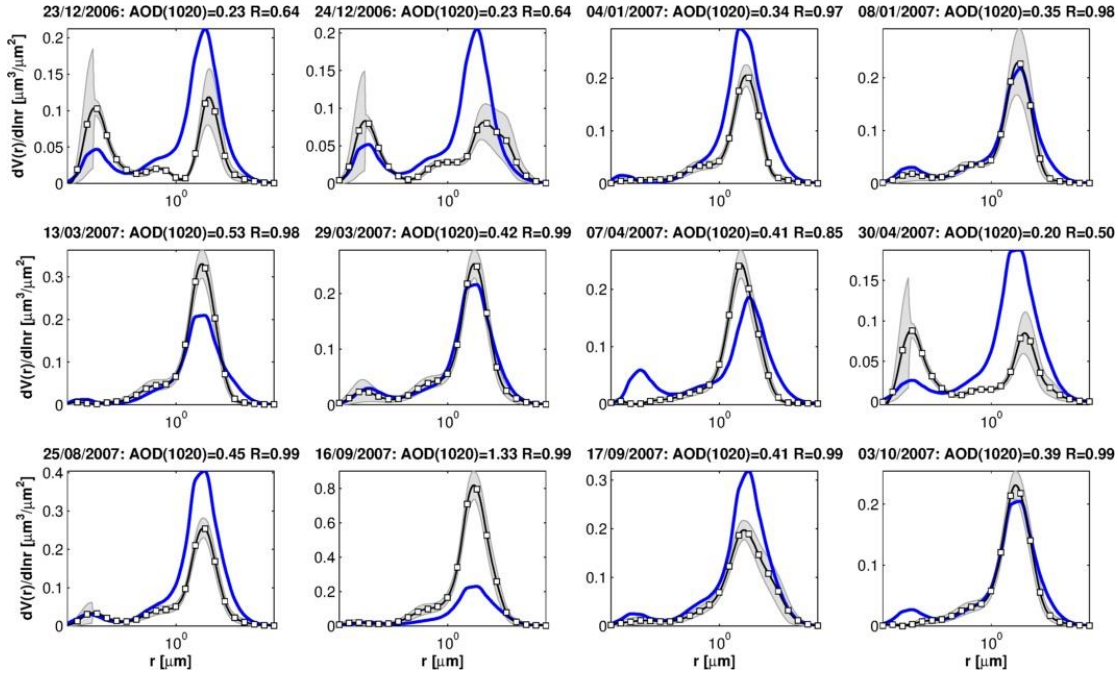

Figure S2.6. Comparison of the spline-fit NN retrieval (blue) and the AERONET daily AVSD retrieval at Dakar (squares overlaid on a spline-fit) for days 61-72 of the test dataset. The estimated error on the AERONET data is shown by the shaded grey band.

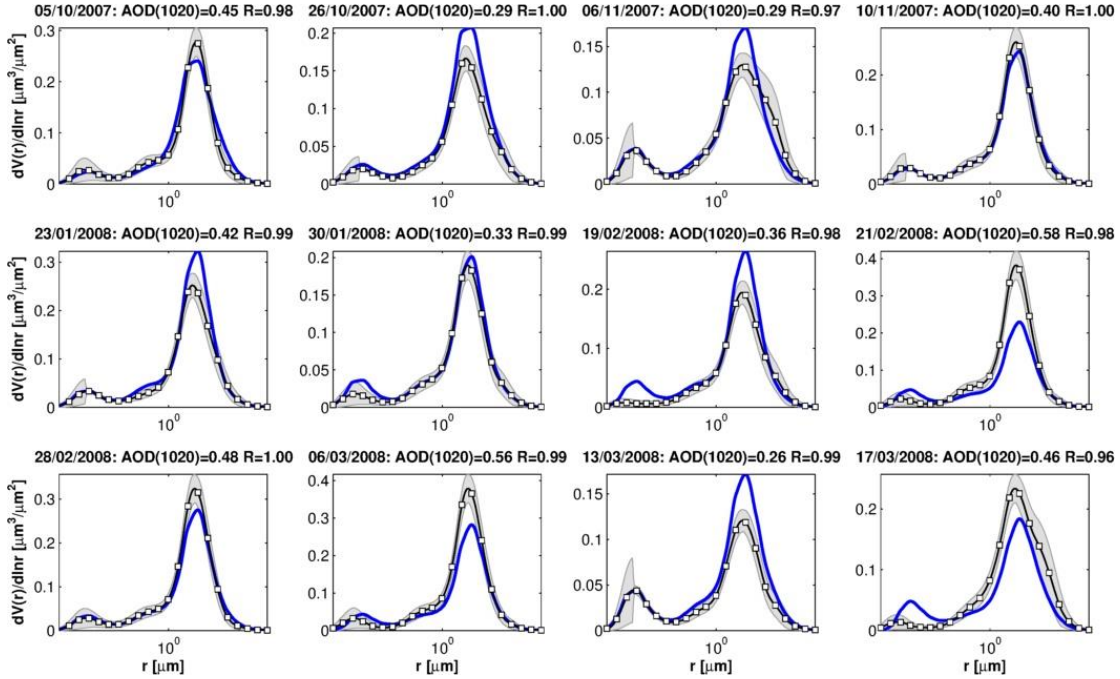

Figure S2.7. Comparison of the spline-fit NN retrieval (blue) and the AERONET daily AVSD retrieval at Dakar (squares overlaid on a spline-fit) for days 73-84 of the test dataset. The estimated error on the AERONET data is shown by the shaded grey band.

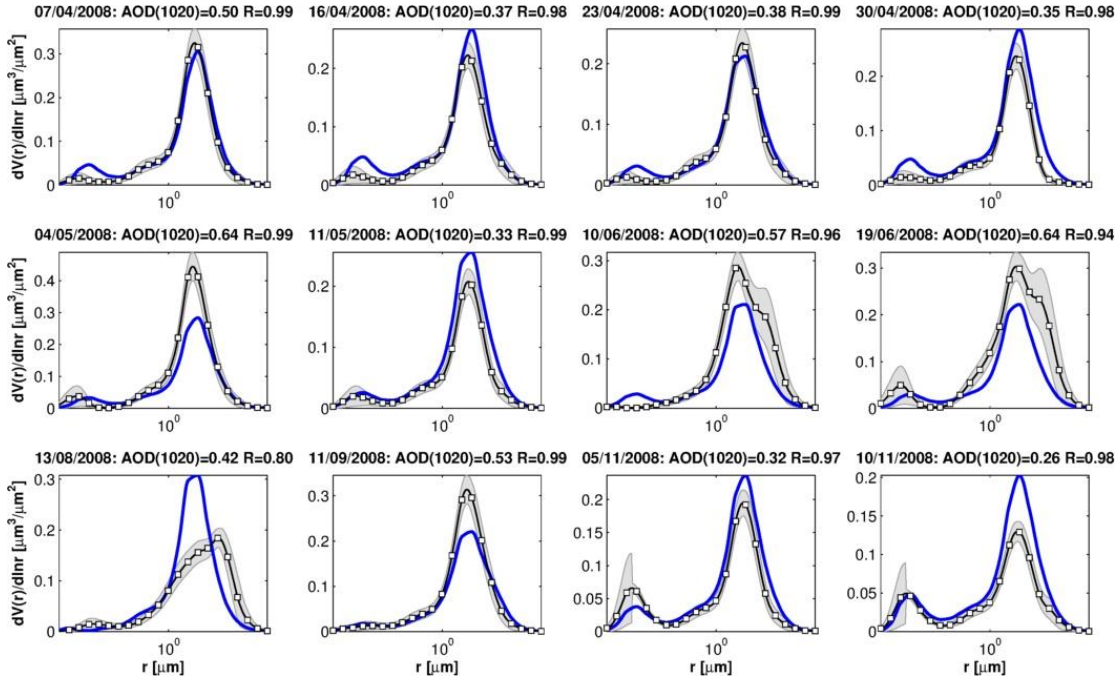

Figure S2.8. Comparison of the spline-fit NN retrieval (blue) and the AERONET daily AVSD retrieval at Dakar (squares overlaid on a spline-fit) for days 85-96 of the test dataset. The estimated error on the AERONET data is shown by the shaded grey band.

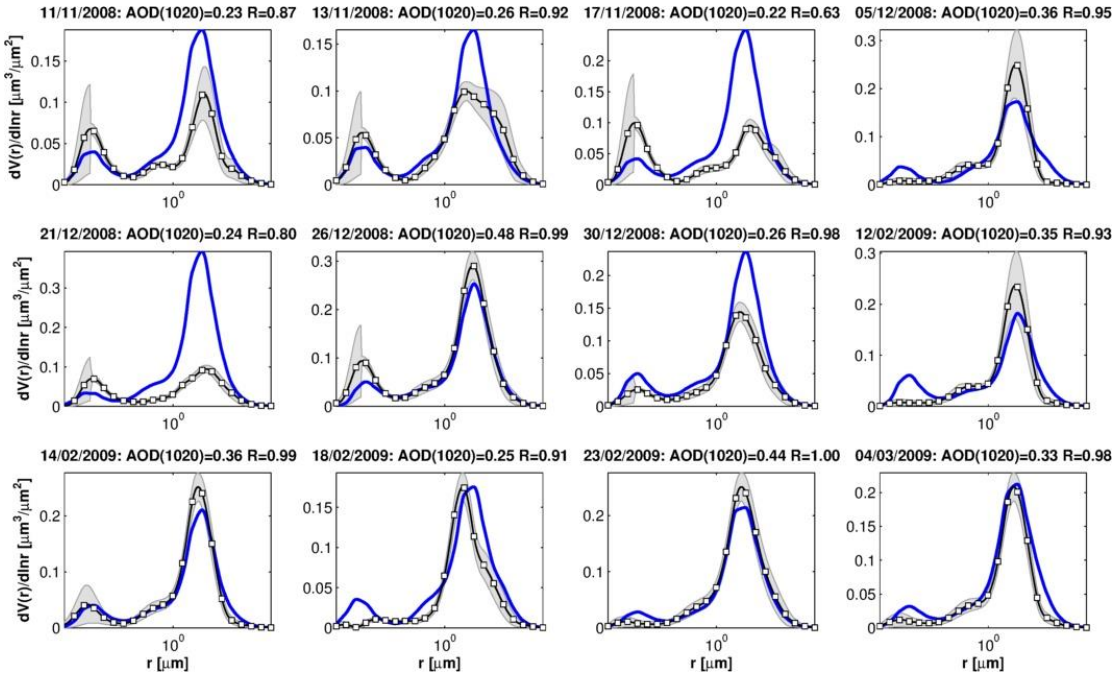

Figure S2.9. Comparison of the spline-fit NN retrieval (blue) and the AERONET daily AVSD retrieval at Dakar (squares overlaid on a spline-fit) for days 97-108 of the test dataset. The estimated error on the AERONET data is shown by the shaded grey band.

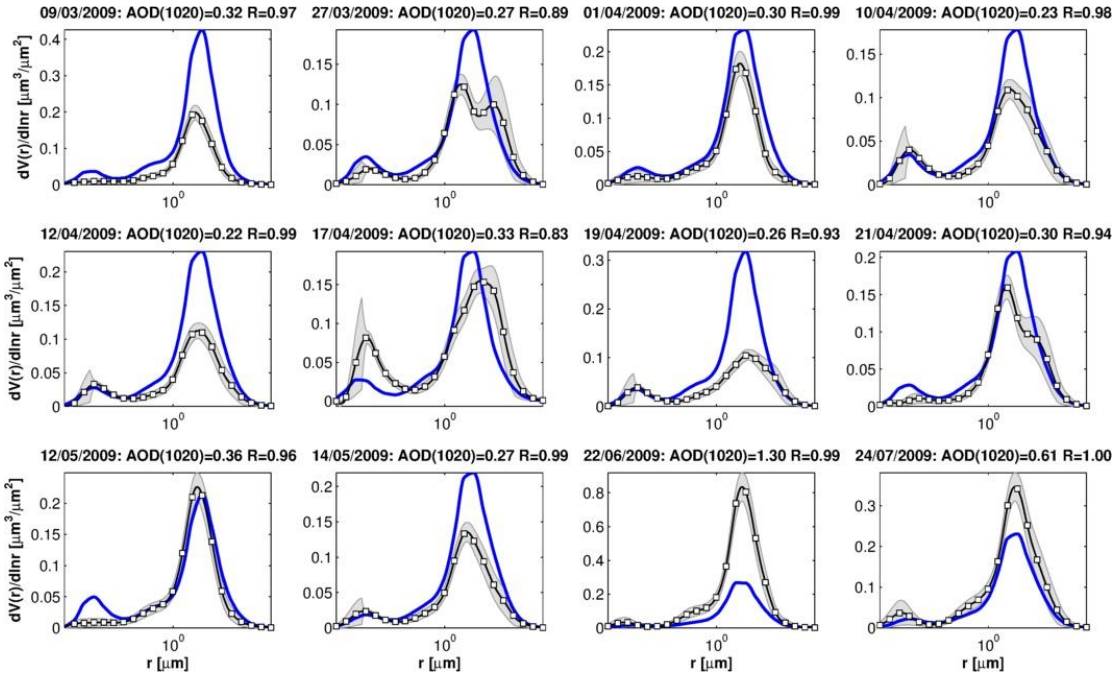

Figure S2.10. Comparison of the spline-fit NN retrieval (blue) and the AERONET daily AVSD retrieval at Dakar (squares overlaid on a spline-fit) for days 109-120 of the test dataset. The estimated error on the AERONET data is shown by the shaded grey band.

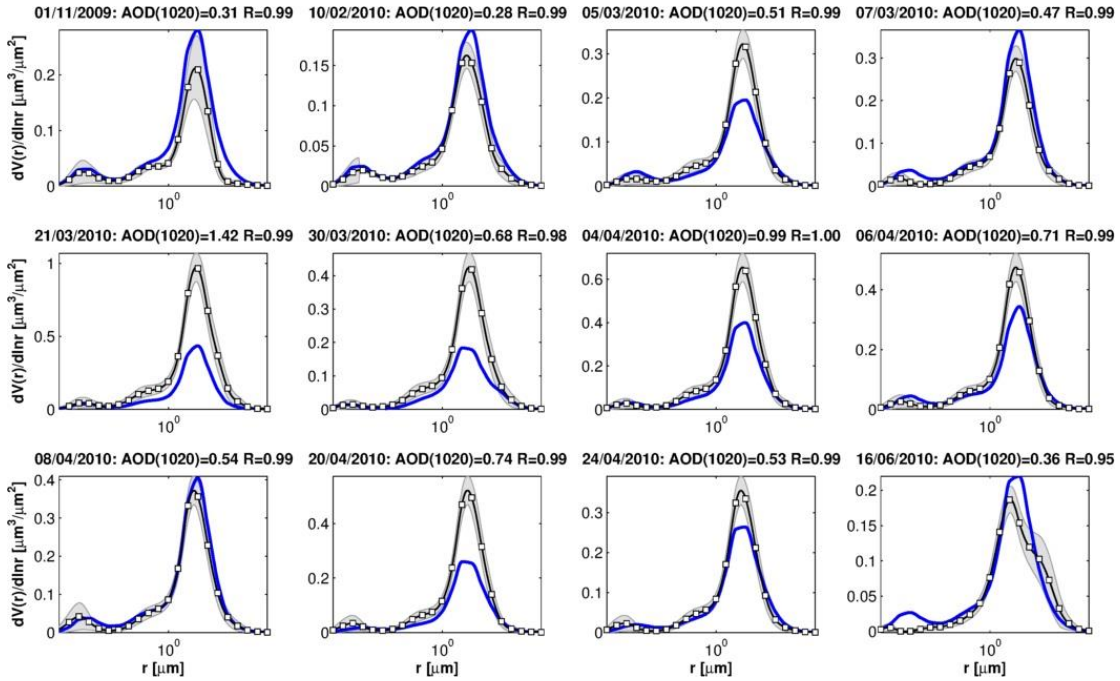

Figure S2.11. Comparison of the spline-fit NN retrieval (blue) and the AERONET daily AVSD retrieval at Dakar (squares overlaid on a spline-fit) for days 121-132 of the test dataset. The estimated error on the AERONET data is shown by the shaded grey band.

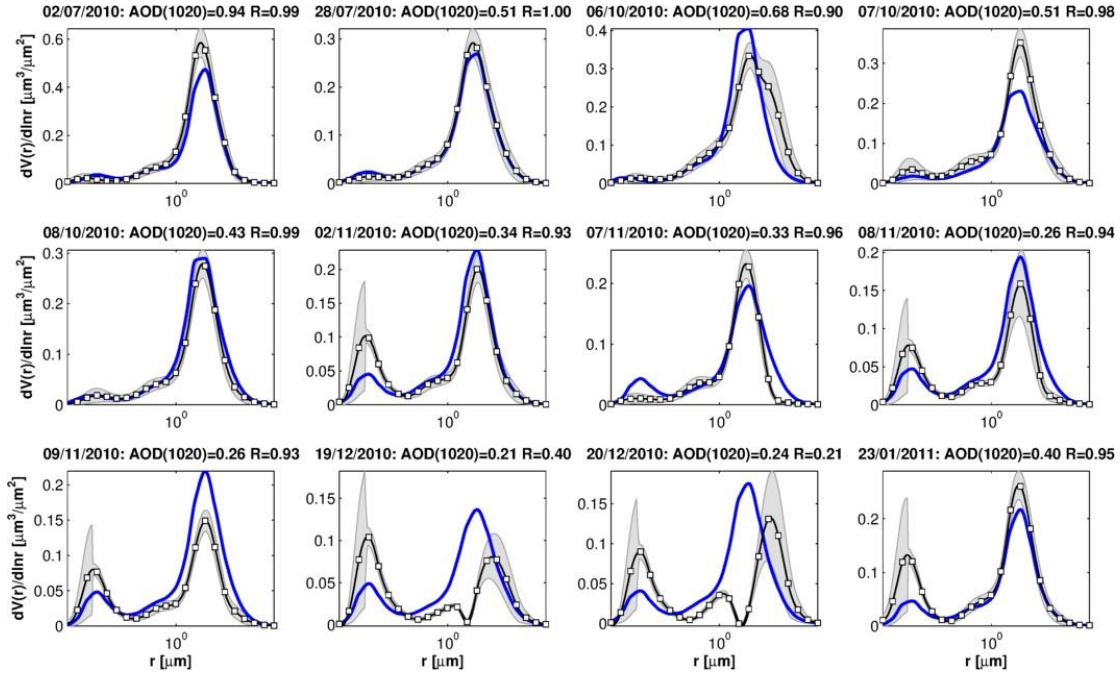

Figure S2.12. Comparison of the spline-fit NN retrieval (blue) and the AERONET daily AVSD retrieval at Dakar (squares overlaid on a spline-fit) for days 133-144 of the test dataset. The estimated error on the AERONET data is shown by the shaded grey band.

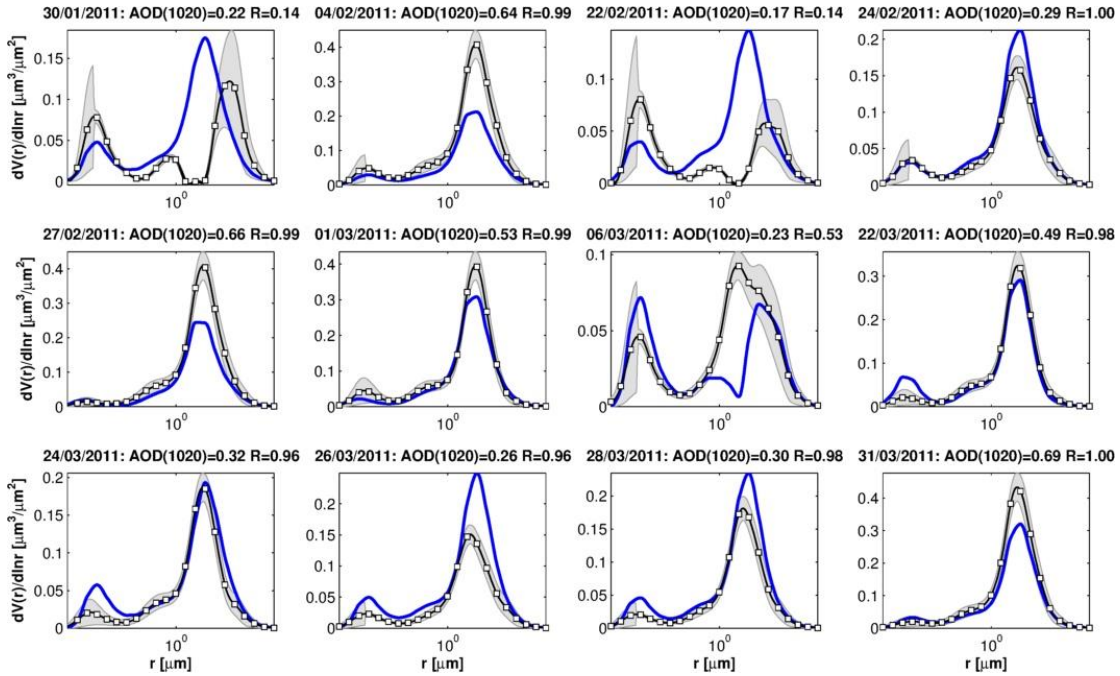

Figure S2.13. Comparison of the spline-fit NN retrieval (blue) and the AERONET daily AVSD retrieval at Dakar (squares overlaid on a spline-fit) for days 145-156 of the test dataset. The estimated error on the AERONET data is shown by the shaded grey band.

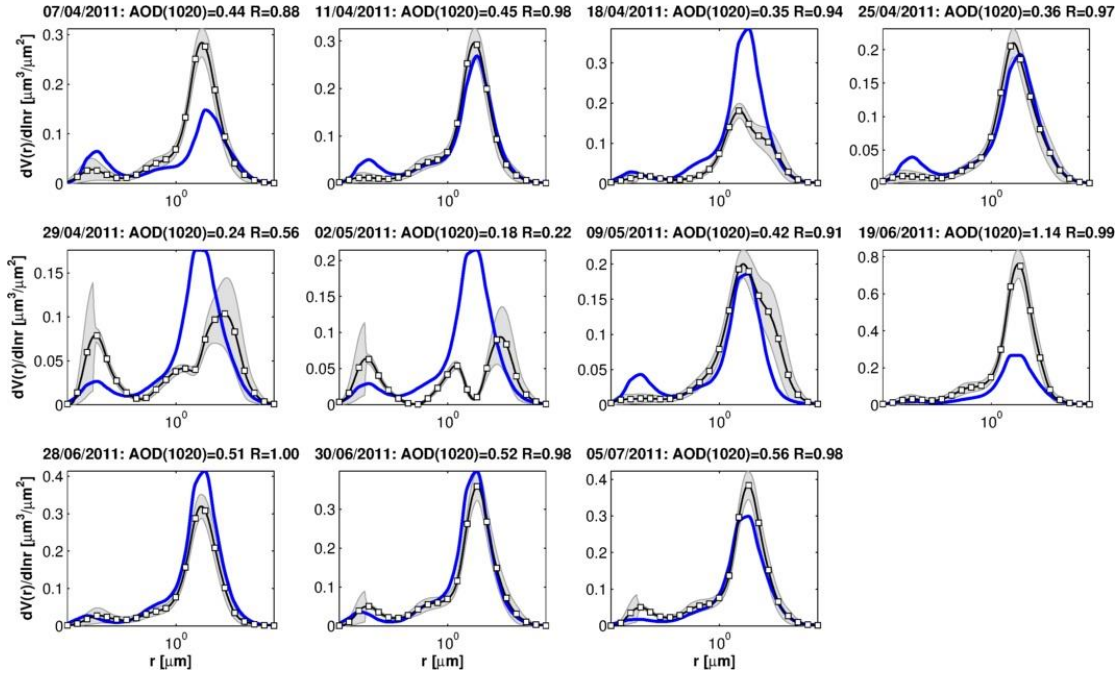

Figure S2.14. Comparison of the spline-fit NN retrieval (blue) and the AERONET daily AVSD retrieval at Dakar (squares overlaid on a spline-fit) for days 157-167 of the test dataset. The estimated error on the AERONET data is shown by the shaded grey band.

S3 Retrieval of climatological means

S3.1 Retrieval of the climatological mean for microphysical secondary parameters

In order to demonstrate that the NN is able to retrieve the climatological mean for the secondary microphysical parameters derived from the AVSD, Fig. S3.1 below compares the

mean of the AERONET Level 2 (Version 2) retrieved values at Dakar with those obtained from the NN retrieval obtained with co-located and synchronous satellite inputs over Dakar.

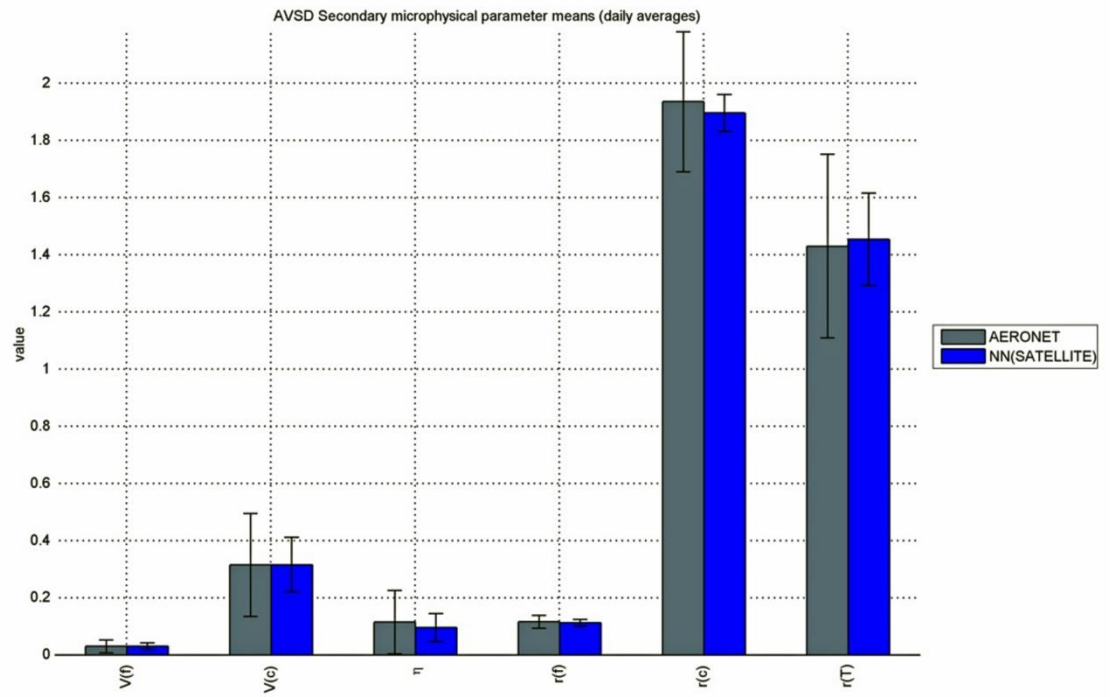

Figure S3.1. Comparison of the climatological mean values of secondary microphysical parameters derived from the AVSD for the NN retrieval and the AERONET daily AVSD retrieval at Dakar. The error bars show one standard deviation of variability in the data.

S3.2 Retrieval of the climatological mean for spectral optical parameters

In order to demonstrate that the NN is able to retrieve the spectral climatological mean for the optical parameters, Fig. S3.2 below compares the spectral mean of the AERONET Level 2 (Version 2) retrieval at Dakar with the uncertainty level identified by Mishchenko (2007) where available, together with the spectral mean of the NN retrieval obtained with co-located and synchronous satellite inputs over Dakar.

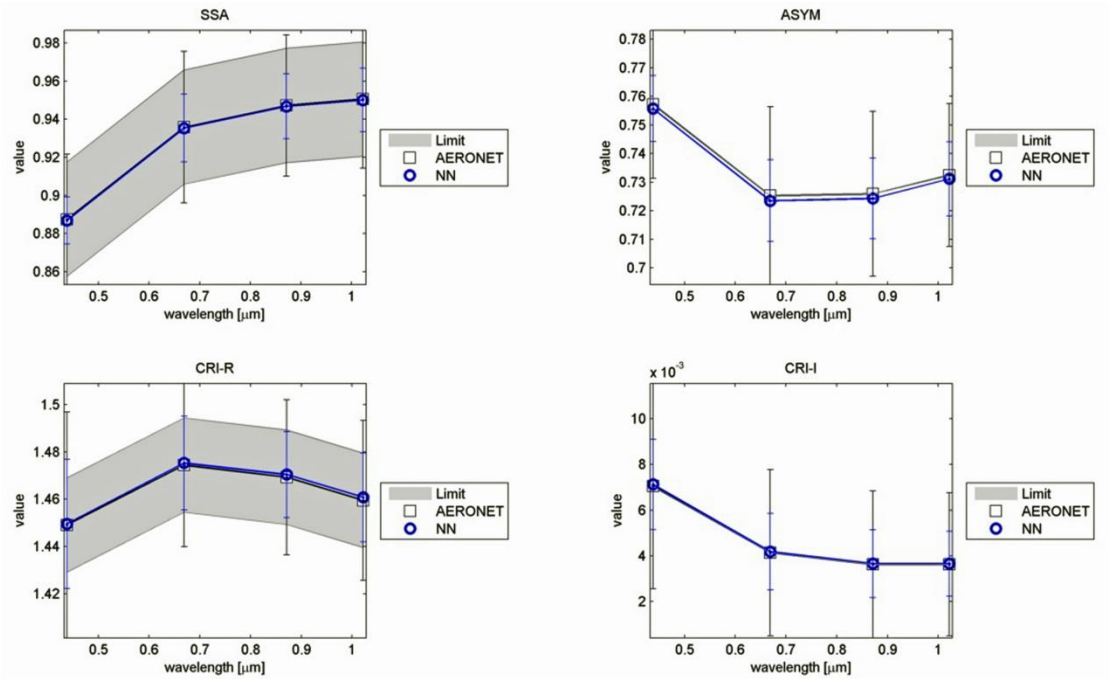

Figure S3.2. Comparison of the climatological mean spectral optical parameters from the NN retrieval and the AERONET daily AVSD retrieval at Dakar. The grey shaded band is the limit of acceptable uncertainty identified by Mishchenko (2007).

S4 Retrieval of spectral optical parameters at timescales from 1-dy to 1-yr

In order to assess the performance of the NN retrieval at Dakar at different timescales, Figs. S4.1-S4.4 below show the variation of the median absolute error (MAE) with respect to the AERONET retrieval of the spectral SSA, CRI and ASYM at the daily, weekly, monthly, seasonally and yearly timescale overlaid on a spline-fit.

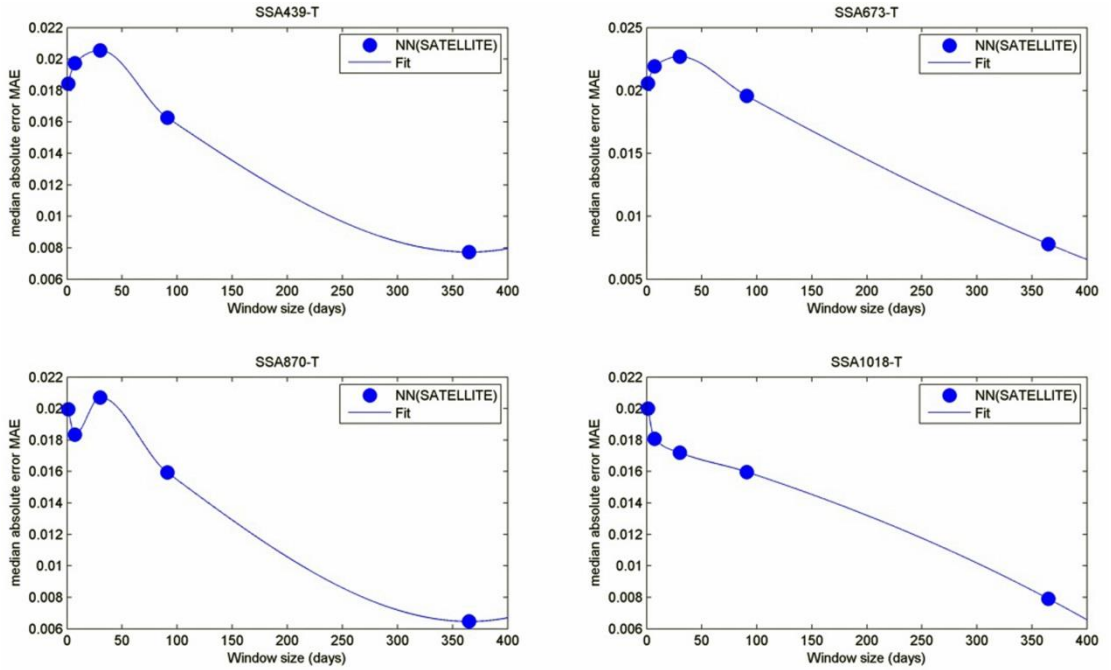

Figure S4.1. Variation of the median absolute error (MAE) with respect to the AERONET retrieval of the spectral SSA at the daily, weekly, monthly, seasonally and yearly timescale overlaid on a spline-fit.

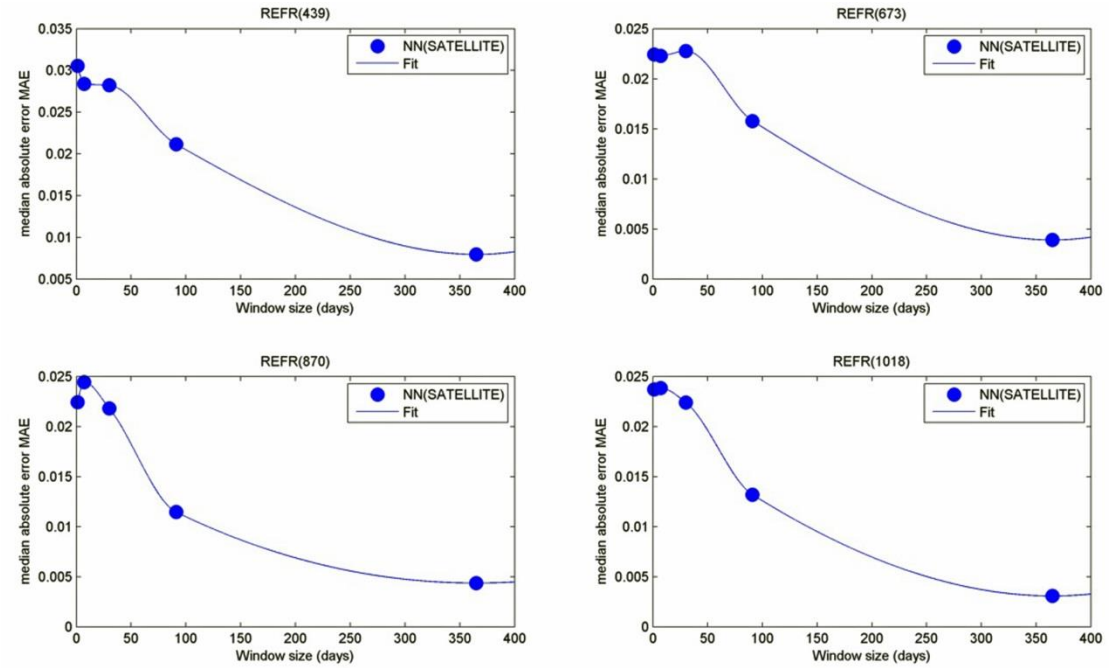

Figure S4.2. Variation of the median absolute error (MAE) with respect to the AERONET retrieval of the spectral CRI-R at the daily, weekly, monthly, seasonally and yearly timescale overlaid on a spline-fit.

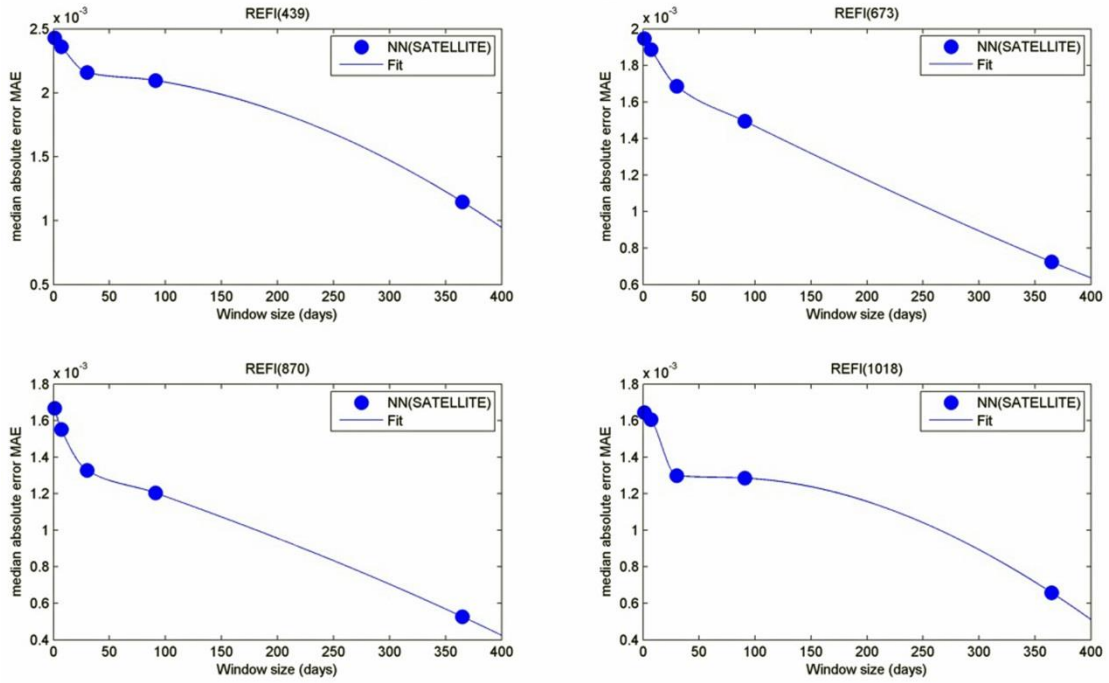

Figure S4.3. Variation of the median absolute error (MAE) with respect to the AERONET retrieval of the spectral CRI-I at the daily, weekly, monthly, seasonally and yearly timescale overlaid on a spline-fit.

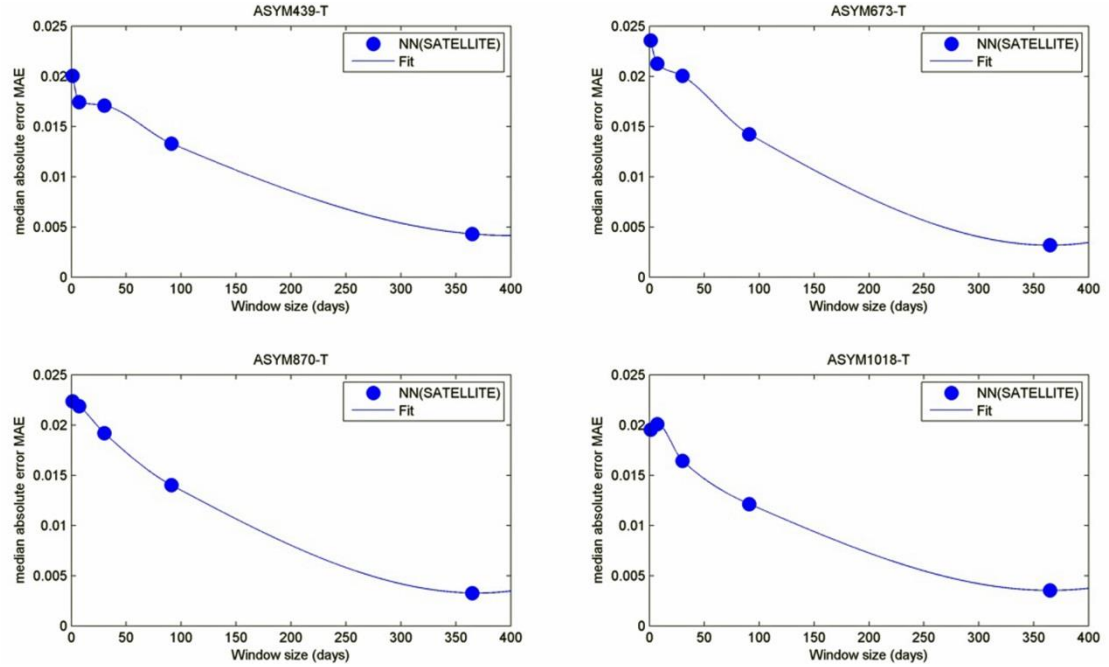

Figure S4.4. Variation of the median absolute error (MAE) with respect to the AERONET retrieval of the spectral ASYM at the daily, weekly, monthly, seasonally and yearly timescale overlaid on a spline-fit.

References

Mishchenko, M. I., Cairns, B., Kopp, G., Schueler, C. F., Fafaul, B. A., Hansen, J. E., Hooker, R. J., Itchkawich, T., Maring, H. B., and Travis, L. D.: Accurate monitoring of terrestrial aerosols and total solar irradiance: introducing the Glory mission, B. Am. Meteorol. Soc., 88, 677–691, 2007.

Taylor, M., Kazadzis, S., and Gerasopoulos, E.: Multi-modal analysis of aerosol robotic network size distributions for remote sensing applications: dominant aerosol type cases, Atmos. Meas. Tech., 7, 839–858, doi:10.5194/amt-7-839-2014, 2014.